

Effect of Humic Acid on the Kinetics of Silver Nanoparticle Sulfidation

Basilius Thalmann^{a,b}, Andreas Voegelin^a, Eberhard Morgenroth^{a,b} and Ralf Kaegi^{a}*

^a Eawag, Swiss Federal Institute of Aquatic Science and Technology, Überlandstrasse 133, CH-8600 Dübendorf

^b ETH Zürich, Institute of Environmental Engineering, CH-8093 Zürich, Switzerland

* Ralf.kaegi@eawag.ch

16 pages, 11 Figures, 4 Tables

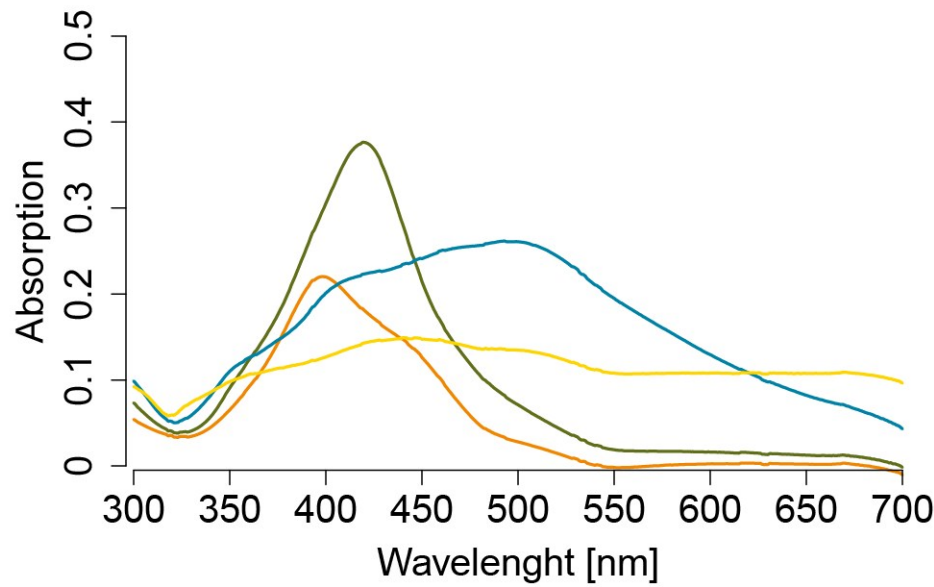


Figure S1. Plasmon resonance of 20-nm (orange), 40-nm (green), 100-nm (blue) and 200-nm (yellow) AgNP.

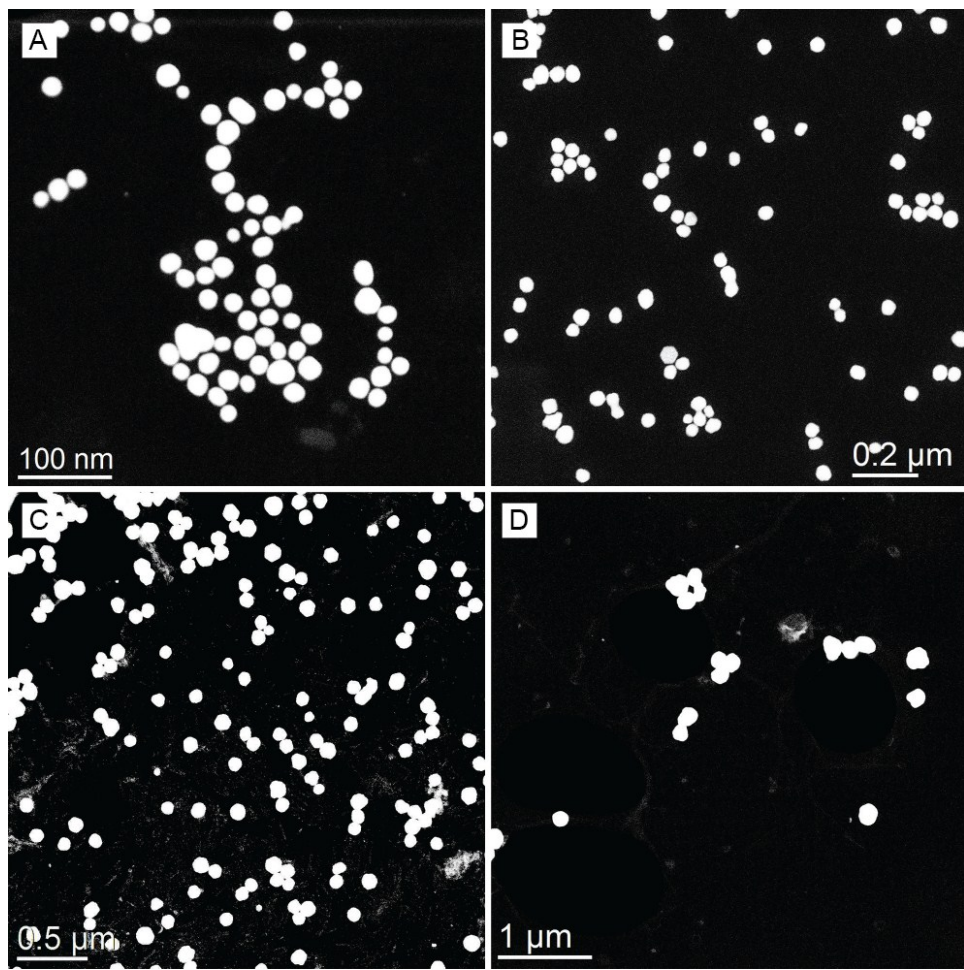


Figure S2. TEM images of pristine AgNP with diameters of 20 (A), 40 (B), 100 (C) and 200 nm

(D).

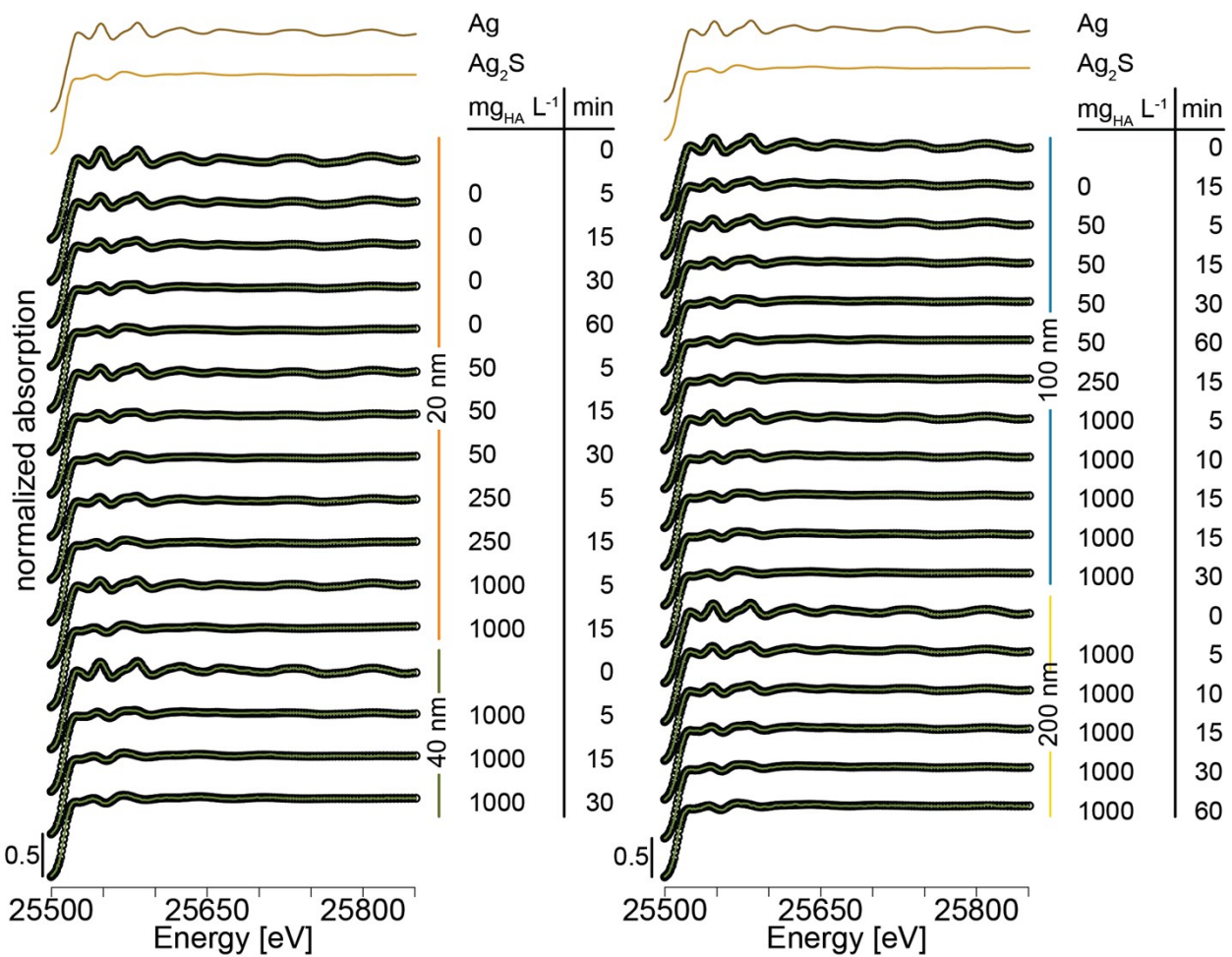


Figure S3. XANES spectra of reference and experimental samples and reconstructed LCF spectra (open circles) using Ag and Ag₂S as reference spectra. For clarity the spectra are plotted with an offset of 0.5. The sum of all fractions was unconstrained for LCF analysis. A comparison of the LCF-derived Ag fraction from XANES and EXAFS is given in **Figure S5**.

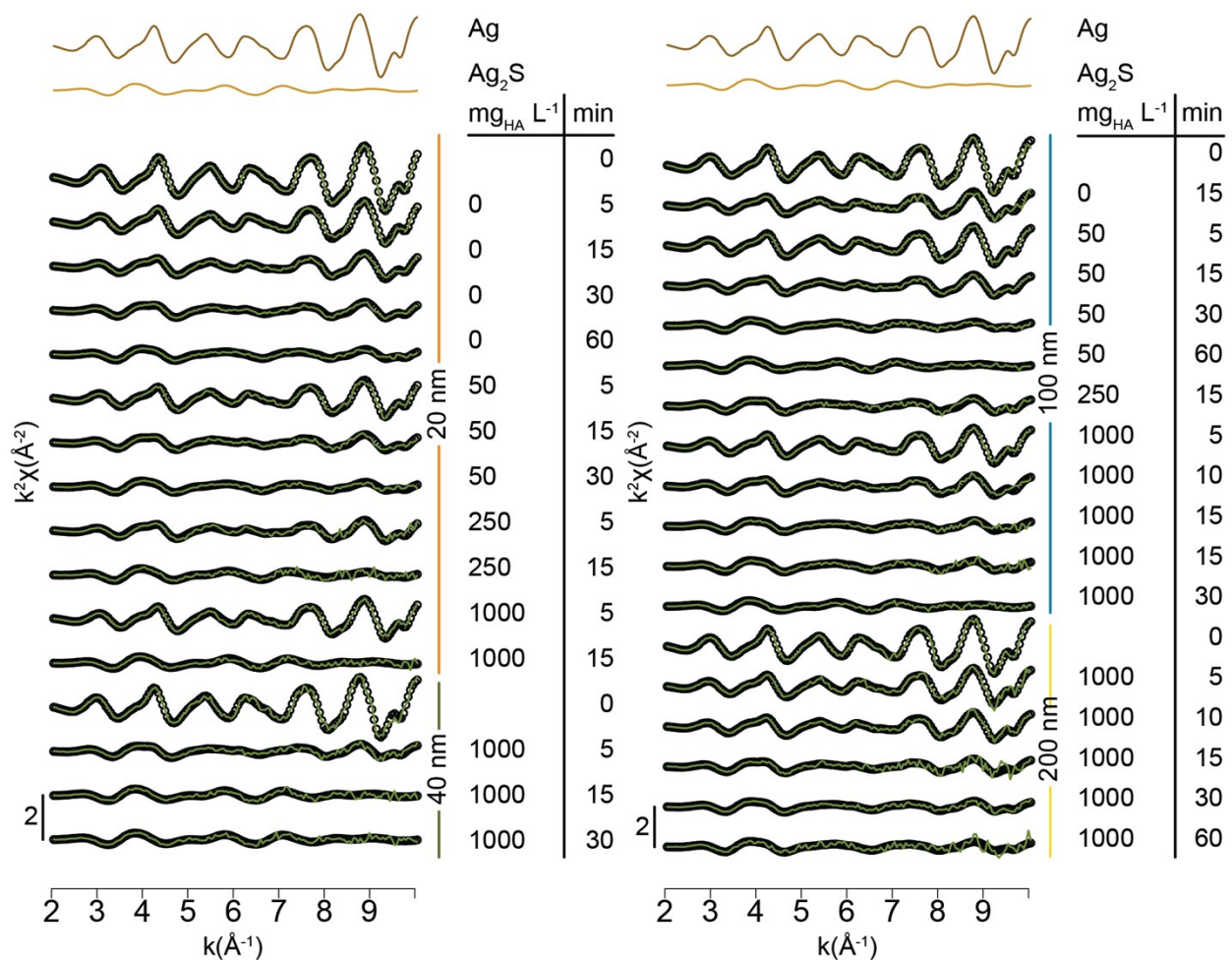


Figure S4. EXAFS spectra of reference and experimental samples and reconstructed LCF spectra (open circles) using Ag and Ag₂S as reference spectra. For clarity the spectra are plotted with an offset of 2. The sum of all fractions was unconstrained for LCF analysis. A comparison of the LCF-derived Ag fraction from XANES and EXAFS is given in **Figure S5**.

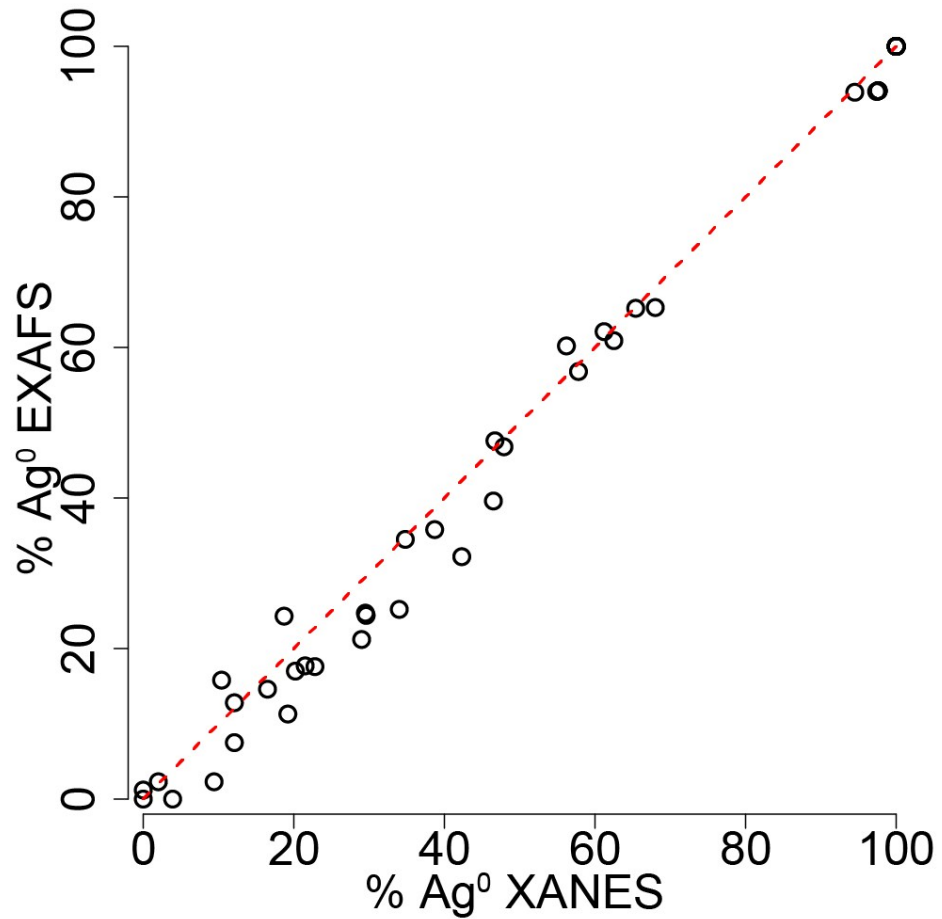


Figure S5. Comparison of the metallic Ag fractions derived from LCF analysis of XANES and EXAFS spectra.

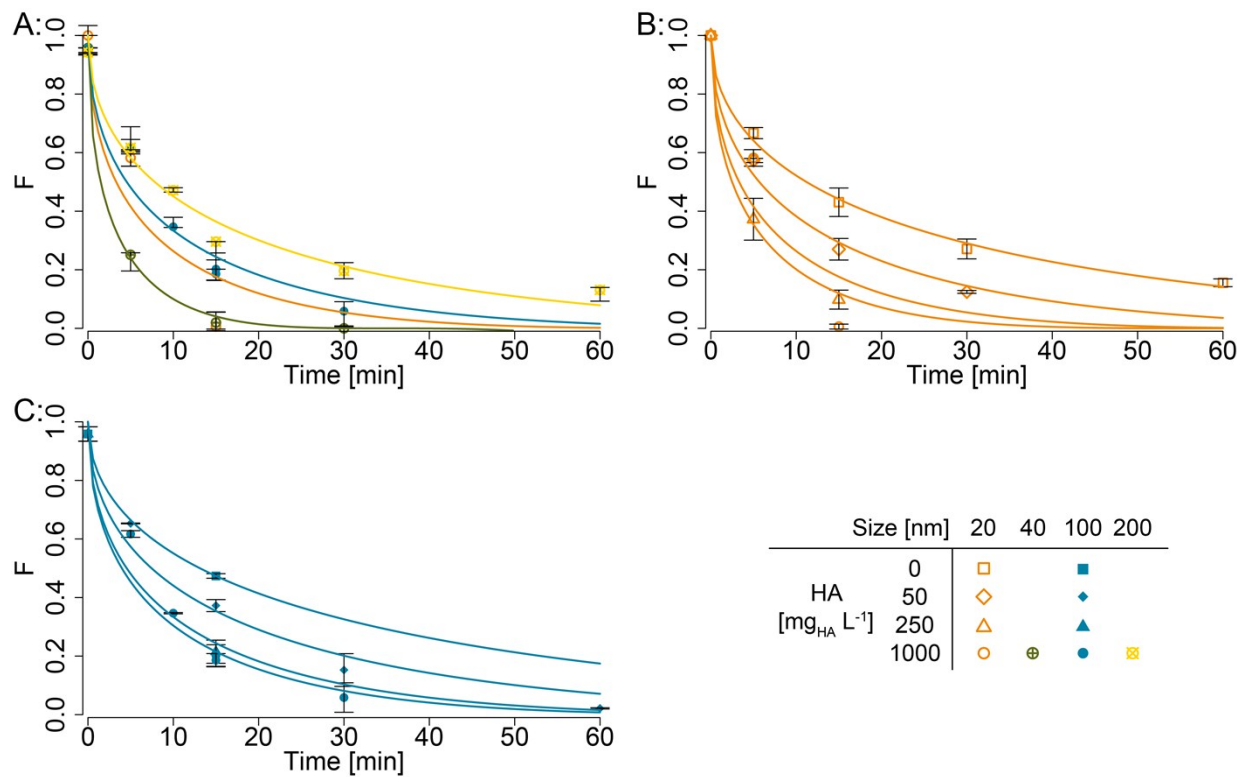


Figure S6. Results of the parabolic rate model fit (lines) to the experimental data (A: AgNP sizes at constant HA concentration, B: 20-nm AgNP at differing HA concentrations, C: 100-nm AgNP at differing HA concentrations).

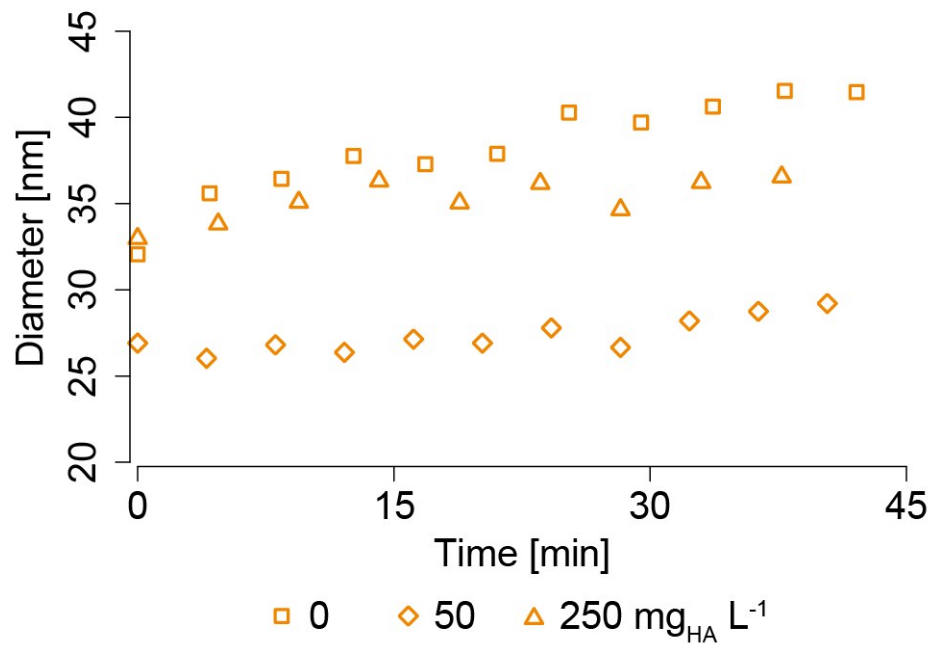


Figure S7. Hydrodynamic diameter measured by DLS over time for 20-nm AgNP in the presence of HA (0, 50 and 250 mg_{HA} L⁻¹, squares, diamonds and triangles respectively) and HS- (2.5 mM).

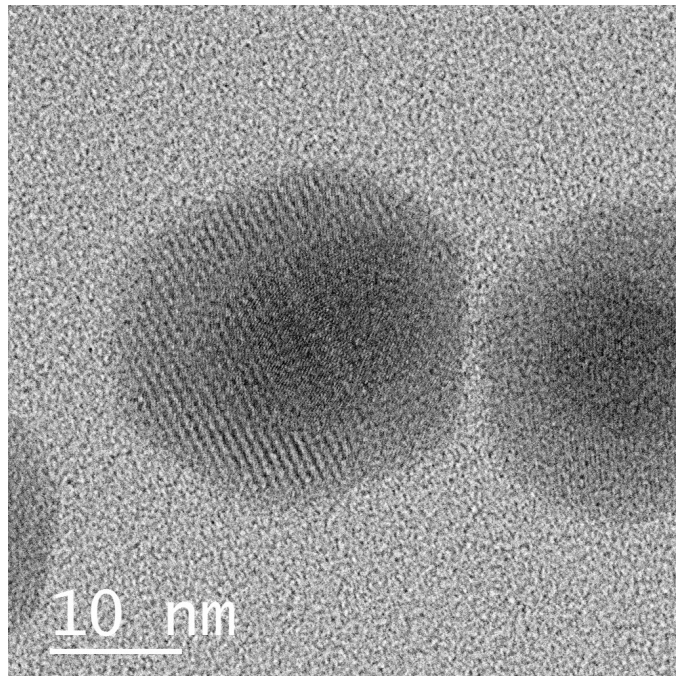


Figure S8. High resolution TEM image of two 20-nm AgNP sulfidized for 5 min in the presence of $250 \text{ mg}_{\text{HA}} \text{ L}^{-1}$. A core-shell type structure is visible.

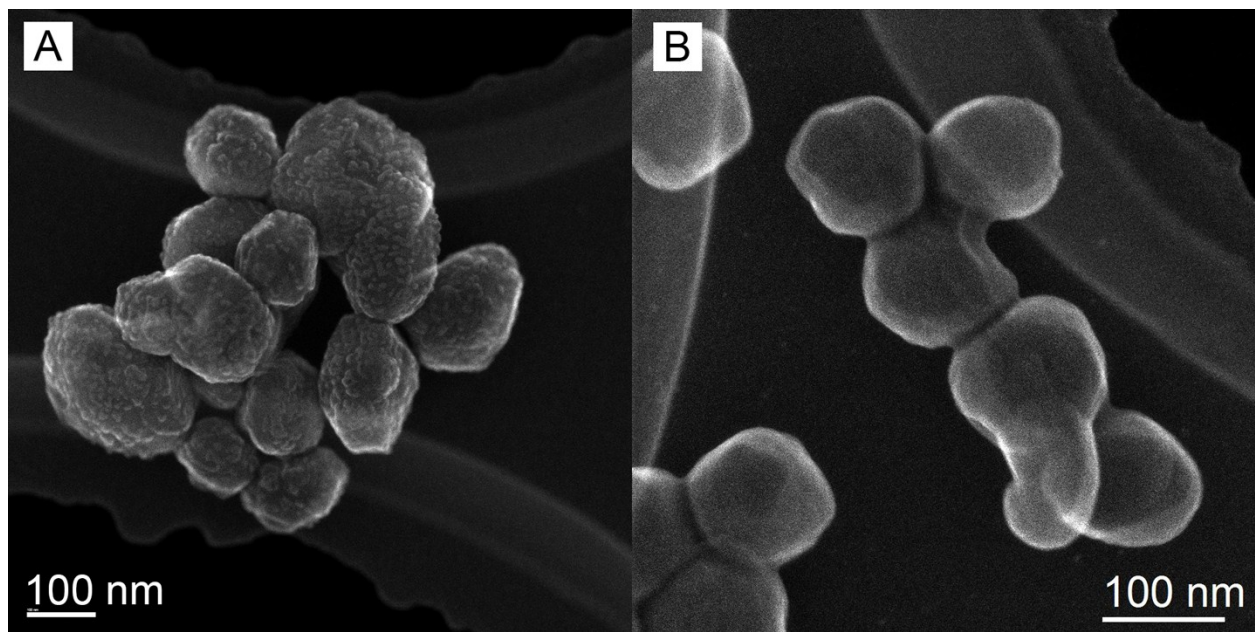


Figure S9. Secondary electron (SE) image of 100-nm AgNP after **A:** 5 min sulfidation in presence of $1000 \text{ mg}_{\text{HA}} \text{ L}^{-1}$ and **B:** after 4 h sulfidation without HA.

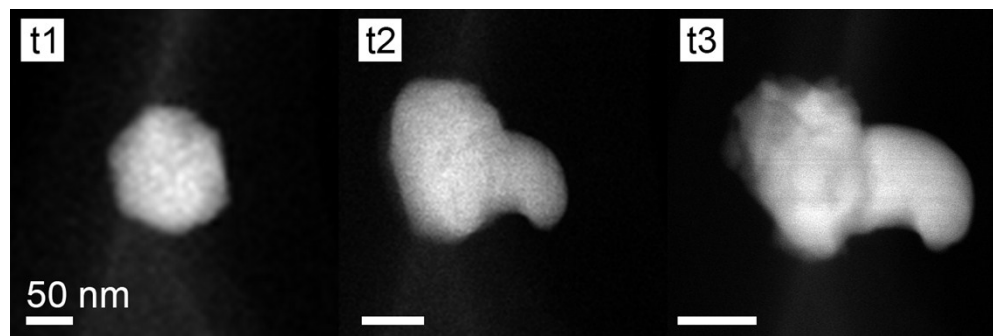


Figure S10. Time sequence of partially sulfidized 100-nm AgNP (15 min with $1000 \text{ mg}_{\text{HA}} \text{ L}^{-1}$) over hundred seconds under the electron beam ($t1 = 0\text{s}$, $t2 = 38\text{s}$ $t3 = 96\text{s}$).

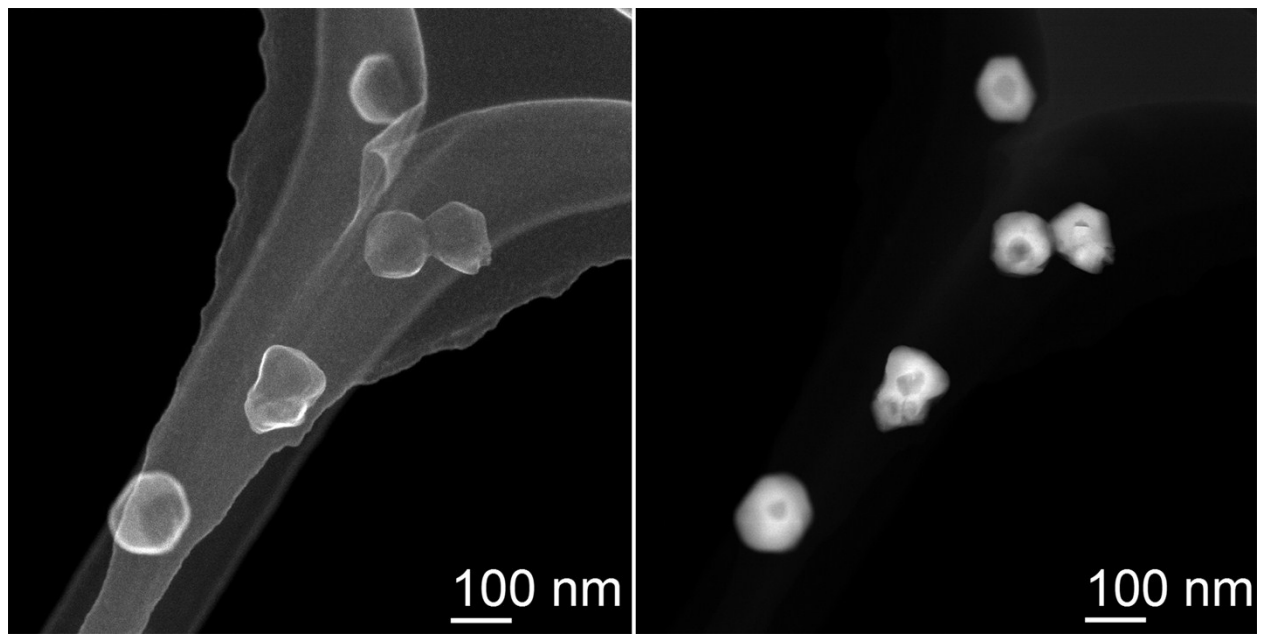


Figure S11. TEM secondary-electron (SE) image of 100-nm AgNP after 15 min reaction with HS⁻ in the presence of 1000 mg_{HA} L⁻¹ (left). Corresponding TEM image of the same particles recorded with HAADF detector (right).

Table S1. AgNP characteristics

	DLS Size [nm] (PDI) ^{a,b}	zeta potential [mV] ^b	TEM Size [nm] (particles sized) ^c
20-nm AgNP	29.33 (0.285)	-40.43	19.0±3.7 (465)
40-nm AgNP	39.44 (0.189)	-42.47	38.2±5.0 (446)
100-nm AgNP	103.7 (0.22)	-48.7	92±14 (153)
200-nm AgNP	228.8 (0.234)	-52.47	207±34 (68)

^a: PDI = Polydispersity Index

^b: 100 ppm AgNP measured in 10 mM HEPES buffer at pH 7.5

^c: 10 ppm AgNP measured in 10 mM HEPES buffer and 2 mM citrate at pH 7.5

Table S2. Summary of Sulfidation Experiments Conducted and Investigated with XAS (X) and TEM (T).

[mg _{H_A} L ⁻¹]	0 min				5				10				15				30				45				60				4h			
	0	50	250	1000	0	50	250	1000	1000	0	50	250	1000	0	50	250	1000	0	50	1000	0	250	0	50	1000	0						
200 nm	XT	X	X	X	XT	X	XT	X		X	X	X	X	X	X	X	T	T	X													
100 nm	T			X				X					X			X																
40 nm																																
20 nm	XT	X	X	X	T	X		XT	X	X	X	X	XT			X	X								X		T					
	T			X				X	X				X			X										X						

Table S3. Average of the LCF Derived Ag Fraction from XANES and EXAFS for Each Measured Sample with Standard Error (σ).

AgNP					AgNP				
Size [nm]	HA [mg _{HA} L ⁻¹]	Time [min]	F _{Ag}	σ	Size [nm]	HA [mg _{HA} L ⁻¹]	Time [min]	F _{Ag}	σ
20	0	0	1.000	0.000	100	0	0	0.959	0.025
20	0	5	0.667	0.019	100	0	15	0.474	0.008
20	0	15	0.431	0.049	100	50	0	0.959	0.025
20	0	30	0.271	0.034	100	50	5	0.653	0.001
20	0	60	0.156	0.013	100	50	15	0.373	0.021
20	50	0	1.000	0.000	100	50	30	0.153	0.056
20	50	5	0.573	0.007	100	50	60	0.022	0.002
20	50	15	0.270	0.037	100	250	0	0.959	0.025
20	50	30	0.125	0.005	100	250	15	0.215	0.040
20	250	0	1.000	0.000	100	1000	0	0.959	0.025
20	250	5	0.373	0.071	100	1000	5	0.617	0.011
20	250	15	0.098	0.033	100	1000	10	0.347	0.002
20	1000	0	1.000	0.000	100	1000	15	0.202	0.037
20	1000	5	0.582	0.028	100	1000	15	0.186	0.023
20	1000	15	0.006	0.008	100	1000	30	0.059	0.050
40	1000	0	0.957	0.024	200	1000	0	0.942	0.004
40	1000	5	0.251	0.055	200	1000	5	0.617	0.006
40	1000	15	0.020	0.028	200	1000	10	0.472	0.006
40	1000	30	0.000	0.000	200	1000	15	0.296	0.062
					200	1000	30	0.196	0.027
					200	1000	60	0.131	0.038

Table S4. Rate coefficients of the Parabolic Rate Model with Confidence Intervals of 1σ .

AgNP Size [nm]	20				40	100				200
HA [$\text{mg}_{\text{HA}} \text{ L}^{-1}$]	0	50	250	1000	1000	0	50	250	1000	1000
$k [\text{nm}^2 \text{ s}^{-1}]$	0.34	0.68	1.55	1.16	10.47	6.86	12.08	22.68	19.84	58.27
Standard error (1σ)	0.02	0.05	0.15	0.42	1.08	0.89	1.30	3.22	2.24	5.04